applied sciences

MDPI

Article

IR and Raman Dual Modality Markers Differentiate among Three *bis*-Phenols: BPA, BPS, and BPF

Kuanglin Chao [1,*], Walter Schmidt [1], Jianwei Qin [1], Moon Kim [1] and Feifei Tao [2]

[1] USDA/ARS Environmental Microbial and Food Safety Laboratory, Beltsville Agricultural Research Center, 10300 Baltimore Avenue, Beltsville, MD 20705, USA; walter.schmidt4870@gmail.com (W.S.); jianwei.qin@usda.gov (J.Q.); moon.kim@usda.gov (M.K.)
[2] Department of Agricultural and Biological Engineering, University of Florida, 1741 Museum Road, Gainesville, FL 32611, USA; ftao@ufl.edu
* Correspondence: kevin.chao@usda.gov

Abstract: *bis*-Phenol A (BPA), *bis*-Phenol S (BPS), and *bis*-Phenol F (BPF) are important polymer industry plasticizers. Regulatory measures have restricted the use of BPA in plastic formulations, especially for those which come in contact with food products. Rapid, accurate spectroscopic measurements are required for distinguishing which of the three are present. The *bis*-phenol groups are structurally identical. The second set of *bis*-groups (CH_3-C-CH_3, O=S=O, and H-C-H, respectively) are discretely different chemically, but vibrational modes corresponding to these groups are not unique identifiers, routinely overlapping with wavenumbers present in other members of the set. The dual modality method identifies the specific wavenumbers in which the Infrared (IR) signal is near zero and the Raman relative intensity is maximum, and those in which the Raman signal is minimum and the IR signal is maximum. The normalized intensity ratio between IR and Raman enhances the signal [BPA 10.6 (1508 cm^{-1}); BPS 7.4 (751 cm^{-1}); BPF 5.1 (1100 cm^{-1})]. The ratio between Raman and IR in BPF is also enhanced: 6.3 (845 cm^{-1}). Discerning which specific wavenumbers are most enhanced is experimentally feasible, though not necessarily at present theoretically predictable. This study demonstrates that IR and Raman spectra are not just complimentary, but together they are confirmatory even when the normalized intensity ratios of corresponding wavenumbers are most different.

Keywords: bisphenols; BPA; BPS; BPF; dual modality; IR; Raman

Citation: Chao, K.; Schmidt, W.; Qin, J.; Kim, M.; Tao, F. IR and Raman Dual Modality Markers Differentiate among Three *bis*-Phenols: BPA, BPS, and BPF. *Appl. Sci.* **2024**, *14*, 6064. https://doi.org/10.3390/app14146064

Academic Editor: Kaiqiang Wang

Received: 30 May 2024
Revised: 5 July 2024
Accepted: 10 July 2024
Published: 11 July 2024

1. Introduction

Plastics contain a range of different chemicals. These chemicals are called plasticizers and are added to change and improve the performance and processing of the plastics. Some plasticizers make plastic more flexible; some make it more resistant to heat and sunlight. Bisphenol A (BPA) is an industrial chemical that has been used as a plasticizer in polycarbonate plastics. Polycarbonate plastics are often used in containers that store food and beverages. Research studies have shown that BPA can leach from containers into food or beverages [1–3]. Exposure to BPA is a food safety concern because it has weak estrogenic effects that can be harmful to human health [4–6]. Bisphenol S (BPS) and Bisphenol F (BPF) are BPA analogs that have been identified at low level (10^{-5} M) by adsorption in thiolated beta-cyclodextrin complexes using Surface-Enhanced Raman Spectroscopy (SERS) [7–9]. A common misconception is that products labeled "BPA-Free" are safe for use when in fact they could potentially pose just as much of a food safety risk as products that are not labeled "BPA-free" [10]. Traditional chemical methods for the detection of these chemicals in plastic products (high-performance liquid chromatography, gas chromatography–tandem mass spectrometry, and liquid chromatography coupled to mass spectrometry) require costly instruments, professional operators, and complex extraction processes. Therefore, a rapid

and accurate screening method is needed to detect these chemical additives in plastic and plastic products when present at levels that may not require extraction or pre-concentration.

Spectroscopy is an efficient, sensitive, and highly effective technique for in situ and in-line product screening for chemical and biophysical markers of changes to products. Recent developments and applications of vibrational spectroscopic technologies to authentication issues in agricultural commodities and foods include utilizing (1) Fourier Transform (FT) infrared (IR) and Raman to detect botanical additives and chemical contaminants in food powders [11,12]; (2) FT-near-infrared (NIR) to detect pork adulteration in veal products [13]; (3) FT-Raman to detect whey added to milk powder [14]; (4) NIR to authenticate honey [15]; and (5) FT-IR spectroscopy combined with chemometrics to authenticate functional food oils [16,17].

Both IR and Raman provide unique spectral fingerprints of a chemical. IR and Raman spectral data are routinely reported as complementary, except that distinguishing which spectral lines in either provide the most spectral information on identity is most often unknown. Since they are structural analogs, all three plasticizers (BPA, BPS, and BPF) will have vibrational modes which would be redundant and perhaps indistinguishable from each other. Collecting both IR and Raman spectra signals can provide both fingerprints and a complete cross-comparison of relevant vibrational modes. The objectives of this study are to achieve the following:

1. Identify spectral wavenumbers in which IR and Raman signals for the same vibrational mode are most different in normalized relative intensity.
2. Use these dual-modality data as a marker to determine the most sensitive signal ratio which is specific to BPA, BPS, and BPF.
3. Assign these wavenumbers to vibrational modes characteristic of individual compounds.

2. Materials and Methods

2.1. Plasticizers

BPA ($(CH_3)_2C(C_6H_4OH)_2$), BPS ($O_2S(C_6H_4OH)_2$), and BPF ($CH_2(C_6H_4OH)_2$) were purchased from Millipore Sigma (Milwaukee, WI, USA). The three analytical standards are in solid form and have purity $\geq$98%.

2.2. FT-IR Spectroscopy and Spectral Measurement

A Nicolet iS50 FT-IR spectrometer (Thermo Fisher Scientific Inc., Madison, WI, USA) covering the spectral range of 400 to 4000 cm^{-1} was used for IR spectrum measurement. The FT-IR spectrometer is equipped with a crystal attenuated total reflectance (ATR) device. Prior to measuring samples, the background spectrum was collected for each sample. For IR spectrum acquisition, a small amount (ca. 5 mg) of plasticizer solid was placed in the ATR and pressed by a pointed tip for uniform contact with the ATR crystal to collect the absorbance. Thirty-two scans with a spectral resolution of 8 cm^{-1} were recorded for each sample, and the average spectrum with a total of 3736 data points was saved for further processing. A total of 30 IR spectra (10 replicates $\times$ 3 plasticizers) were collected for IR modality analysis.

2.3. Raman Spectroscopy and Spectral Measurement

A custom-designed point-scan Raman spectroscopy system was used for Raman spectrum measurement. The point-scan Raman system has a 638 nm laser module (I0638MM0100MF, Innovative Photonics Solutions, Plainsboro, NJ, USA) which delivers approximately 100 mW at the sample level. A bifurcated fiber optic Raman probe (RPB638, InPhotonics, Inc., Norwood, MA, USA) was used to focus the laser light on the sample surface and to collect the Raman signals. The system uses a Raman spectrometer (QEPRO-RAMAN-638, Ocean Optics, Orlando, FL, USA) to accommodate Raman spectral acquisition. The spectra were acquired with a 2 s exposure time at a resolution of 8 cm^{-1} and a Raman shift range of

400 cm^{-1} to 3185 cm^{-1}. A total of 30 Raman spectra (10 replicates × 3 plasticizers) were collected for Raman modality analysis.

2.4. Dual-Modality IR and Raman Data Analysis

All the original FTIR and Raman spectra were baseline-corrected and normalized. Origin 2018 software (OriginLab, Northampton, MA, USA) was used for baseline correction and normalization. The baseline was manually set by 6 anchor points. The baseline was composed by drawing a smooth cubic spline curve which was fitted through those anchor points between 400 and 3100 cm^{-1}. This baseline was subtracted from the spectrum to yield the baseline-corrected spectrum. The baseline-corrected spectrum was normalized to the range 0 to 1.

Bond distances, bound angles, and vibrational mode wavenumber assignments were calculated and identified using commercial computational chemistry software (HyperChem 8.0, Hypercube, Inc., Gainesville, FL, USA) and verified using references in the published literature.

3. Results

3.1. IR and Raman Band Assignment

The chemical structures of BPA, BPS, and BPF (Figure 1) identifying the difference among the three *bis*-phenol compounds contain CH_3-C-CH_3, O=S=O, and H-C-H, respectively. The structural difference suggests that bond distance and bond angles among CH_3-C-phenol, O=S-phenol, and H-C-phenol may not be equal. The full-range IR and Raman spectra of BPA (Figure 2) show vibrational modes characteristic of its structure. The vibrational modes for CH_3-C-phenol enable access to the twist of the phenolic ring relative to the CH_3-C- moiety. IR and Raman spectra compared O=S- or H-C- (Figures 3 and 4).

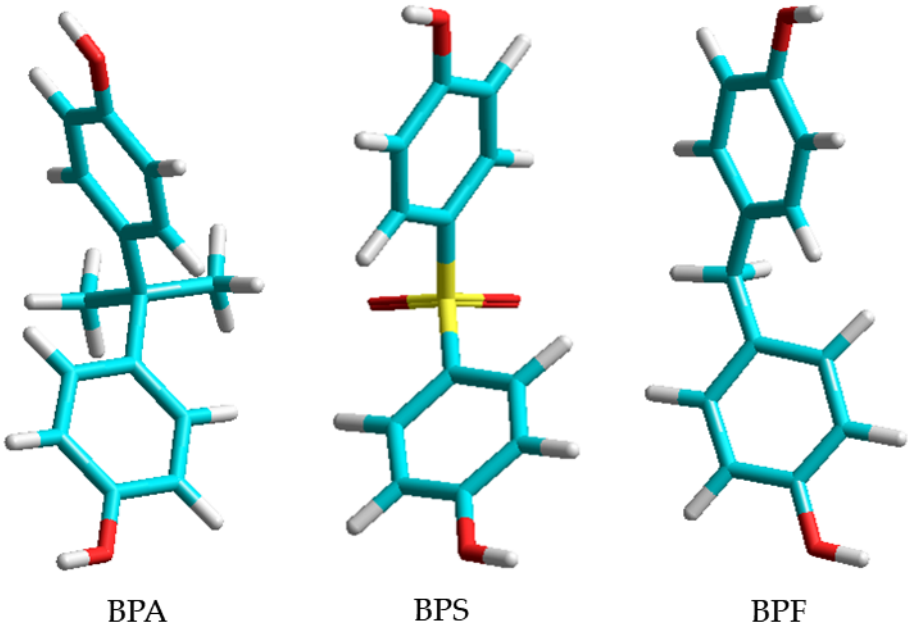

Figure 1. Chemical structure of BPA, BPS, and BPF. Atoms of carbon are light blue, hydrogen white, oxygen red, and sulfur yellow.

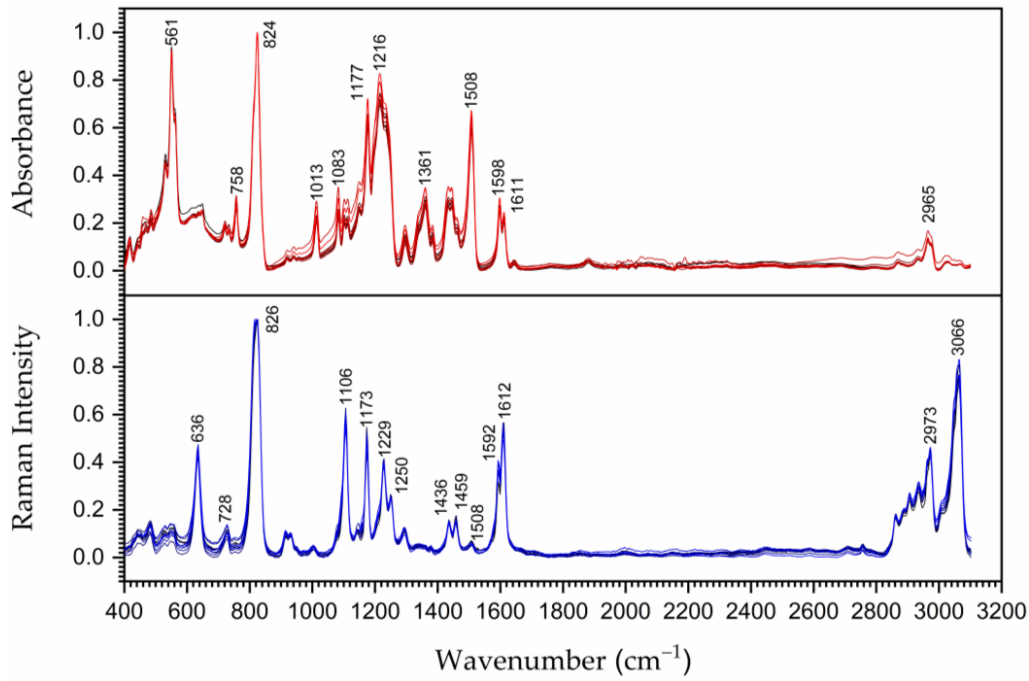

Figure 2. Normalized IR and Raman spectrum measurements on 10 replicates of BPA.

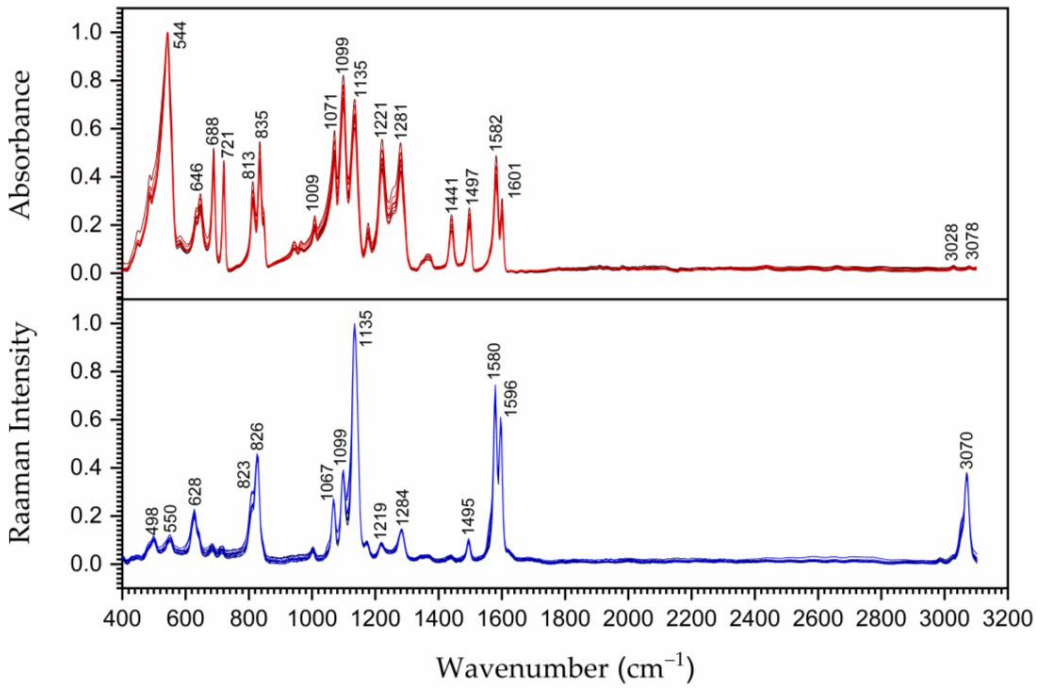

Figure 3. Normalized IR and Raman spectrum measurements on 10 replicates of BPS.

Five IR wavenumbers (2966 cm^{-1}, 1612 cm^{-1}, 1598 cm^{-1}, 1177 cm^{-1}, and 824 cm^{-1}) reasonably match five Raman wavenumbers (2973 cm^{-1}, 1611 cm^{-1}, 1592 cm^{-1}, 1173 cm^{-1}, and 826 cm^{-1}). The two highest intensity peaks unique to IR (1508 cm^{-1} and 561 cm^{-1}) have no corresponding Raman peak at a similar wavenumber. The three largest Raman intensity peaks (3066 cm^{-1}, 1106 cm^{-1}, and 636 cm^{-1}) have virtually no corresponding IR peaks at a similar wavenumber. These five peaks are together a clear fingerprint for confirming BPA. The assignment of wavenumbers to IR and Raman vibrational modes referenced in the literature is shown in Table 1. Grace et al. [18] calculated the wavenumber for 64 different vibrational modes in the phenolic moiety. Observed IR and Raman wavenumbers in BPA

phenolic groups are assigned based on the phenolic group in the article. C-H stretching in CH_3 (IR 2965 cm^{-1}, Raman 2973 cm^{-1}) and CH_3-C-CH_3 scissoring (Raman 1106 cm^{-1} asym) assignments are cited as referenced. The wavenumbers which involve symmetrical vibrational modes are most intense in IR, and those which involve asymmetrical vibrational modes are most intense in Raman.

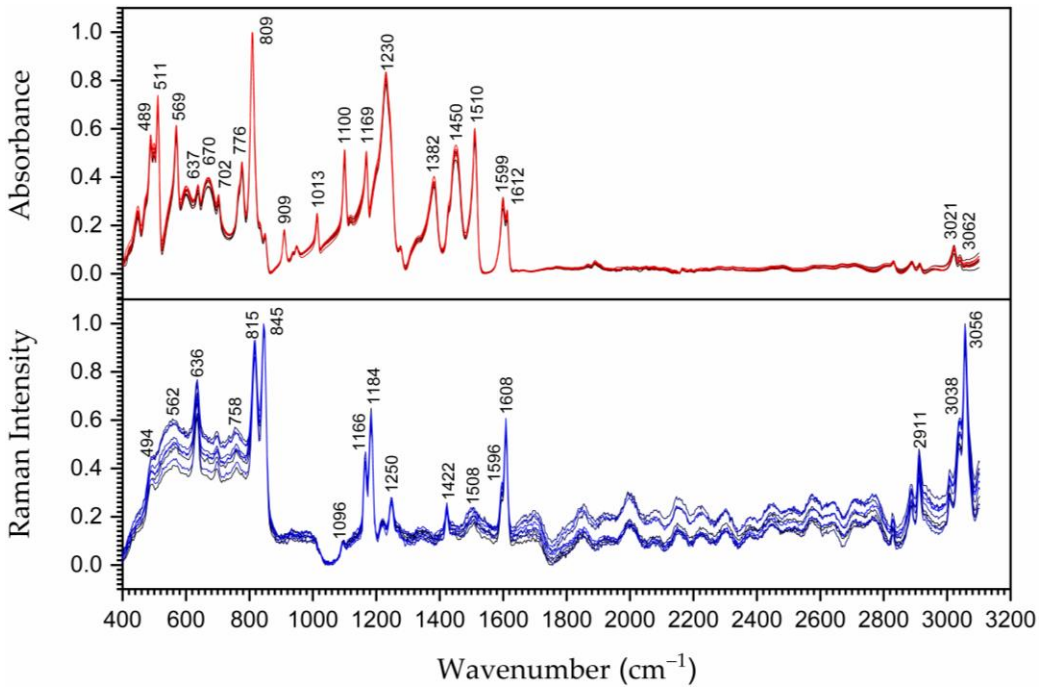

Figure 4. Normalized IR and Raman spectrum measurements on 10 replicates of BPF.

Table 1. Vibrational mode assignments of BPA.

Wavenumber (cm^{-1})	IR Assignments	Raman Assignments
561	(C-C-C ip bend)	
636		C-C-C-OH twist
728	C-C-C ip bend	
758		C-C-C-O-H wag
824	C-C-C trigonal bend	
826		C-C-C trigonal bend
1013	C-H oop bend	
1083	C-H twist	
1106		CH_3 scissoring asym
1173		CH_2 twisting
1177	CH_2 twisting	
1216	CH_2 twist + OH bend	
1229		C-H ip bend
1250		C-H bending asym
1361	C-H bending sym	
1436		OH bend asym
1459		CH_3 deformation asym
1508	(C-H ip bend in-phase)	
1592		C=C stretch in phenol asym
1598	C=C stretch in phenol sym	
1611	C=C stretch in phenol sym	
1612		C=C stretch in phenol asym
2965		C-H str in CH_3 asym

Table 1. *Cont.*

Wavenumber (cm^{-1})	IR Assignments	Raman Assignments
2973	C-H str in CH_3 sym	
3066		OH op str asym

ip = in-plane; op = out of plane; oop = out of plane on two adjacent sites; sym = symmetrical mode; asym = asymmetric mode.

The full-range IR and Raman spectra of BPS (Figure 3) show vibrational modes characteristic of its structure. The vibrational modes for O-S-phenol enable access to the tilt of the phenolic ring relative to the O=S- moiety. In this data set, the relative intensity of corresponding wavenumbers is the major difference between IR and Raman spectra. The IR wavenumbers (1601 cm^{-1}, 1582 cm^{-1}, 1497 cm^{-1}, 1281 cm^{-1}, 1221 cm^{-1}, 1335 cm^{-1}, 1099 cm^{-1}, 835 cm^{-1}, and 813 cm^{-1}) reasonably match Raman wavenumbers (3070 cm^{-1}, 1596 cm^{-1}, 1580 cm^{-1}, 1495 cm^{-1}, 1284 cm^{-1}, 1219 cm^{-1}, 1335 cm^{-1}, 1099 cm^{-1}, 826 cm^{-1}, and 823 cm^{-1}). The two highest intensity IR peaks are 544 cm^{-1} and 1099 cm^{-1}, the first of which has no corresponding Raman peak. The three largest peaks unique to Raman (3070 cm^{-1}, 1067 cm^{-1}, and 628 cm^{-1}) have virtually no corresponding IR peaks at a similar wavenumber. These five peaks confirm BPS identity. The assignment of wavenumbers to IR and Raman vibrational modes referenced in the literature is shown in Table 2. Ullah et al. [19] used DFT to calculate the wavenumber of BPS which enabled assignments of structurally unusual C-S stretching in C-SO2 moiety (near 685 cm^{-1}) and S-O stretching (near 1099 cm^{-1}) [20]. Comparisons with wavenumbers and assignments for BPA were also reported. CH_3-C-CH_3 scissoring asym (Raman 1106 cm^{-1} asym) appears in the same spectral range as S-O stretching. The analogous vibrational mode O-S-O scissoring and/or C-S-C (in phenol-S-phenol moiety) scissoring was not specifically assigned or identified. In addition in IR, three sets of paired similar-intensity peaks are present (1497 cm^{-1} and 1441 cm^{-1}; 1281 cm^{-1} and 1221 cm^{-1}; and 721 cm^{-1} and 688 cm^{-1}). No comparable equal-intensity sets of pairing was observed in Raman. One explanation for the IR pairing in BPS is that the vibrational modes site to site on the two phenolic groups are symmetrical, of nearly equal intensity, and in sync in wavenumber but 180 degrees out of phase. One of the IR pairs (1497 cm^{-1} and 1441 cm^{-1}) is in the same spectral range as CH_3 in CH_3-C-CH_3 deformation (1459 cm^{-1}) except that the deformation in BPA is detected in the Raman spectrum and not in the IR spectrum.

The full-range IR and Raman spectra of BPF (Figure 4) assigns vibrational modes characteristic of this bis-phenol structure containing a H2C-phenol moiety which is exactly the same moiety in the side chain of the amino acid tyrosine. The same wavenumbers assigned by Grace et al. [18] to tyrosine include all the vibrational modes for H2C-phenol in BPF. The four highest intensity peaks in IR peaks (809 cm^{-1}, 1230 cm^{-1}, 511 cm^{-1}, and 1510 cm^{-1}) are unique to IR except one (Raman 1508 cm^{-1}). The four highest intensity peaks in Raman (3056 cm^{-1}, 845 cm^{-1}, 815 cm^{-1}, and 1608 cm^{-1}) are predominantly unique to Raman except one (IR 1612 cm^{-1}). The assignments of wavenumbers to vibrational modes are listed in Table 3. Assignments numbering specific ring carbons in the phenolic ring resulting in individually observed wavenumbers are also available in Hernandez et al. [21]. The numbering in BPF is not reported because of the uncertainty of which set of specific sites in each phenolic ring can discerned as identical.

Table 2. Vibrational mode assignments of BPS.

Wavenumber (cm^{-1})	IR Assignments	Raman Assignments
498		O-S-C bend asym
544	O-S-O bend sym	
550		O-S-O bend asym
628		C-C-C-O-H twist asym
646	C-C-C-OH twist sym	
688	S-O stretch sym	
721	H-C-C-C twist	
813	C-C-C-H twist	
823		C-C-C-H twist asym
826		C-C-C trigonal bend asym
835	C-C-C trigonal bend sym	
1009	C-S-C trigonal bend sym	
1067		C-S-C trigonal bend asym
1071	S-O stretch sym	
1099	S-O stretch sym	S-O stretch asym
1135	C-H oop trigonal bend	C-H oop trigonal bend
1219		C-O stretch asym
1221	C-O stretch sym	
1281	C-O stretch sym	
1284		C-O stretch asym
1441	C-S-C deformation sym	
1495		C-S-C deformation asym
1497	C-S-C deformation sym	
1580		C=C stretch in phenol asym
1582	C=C stretch in phenol sym	
1596		C=C stretch in phenol asym
1601	C=C stretch in phenol sym	
3070		OH op stretch

Table 3. Vibrational mode assignments of BPF.

Wavenumber (cm^{-1})	IR Assignments	Raman Assignments
489	C-C-C oop bend	
494		C-C-C oop bend
511	C-C-O-H bend	
562		C-C-C ip bend
569	C-C-C ip bend	
636		C=C-O torsion
670	C-C-C bend + C-H wag	
776	C-C-C bend + O-H wag	
809	C-C-C trigonal bending asym	C-C-C bend + O-H wag
815	**a**	
845	**b**	
909	Ring breathing	C-C-C trigonal bending asym
1013	C-H oop bend) sym	C-C-C trigonal bending asym
1096		
1100	H-C-H scissoring sym	
1166		H-C-H scissoring asym
1169	C-H oop bend sym	
1230	O-H bend + CH_2 twist sym	C-H oop bend asym
1250		
1382	C-H in CH_2 bending	
1422		O-H bend + CH_2 twist asym
1450	H-C-H scissoring sym	
1508		C-O-H bending asym
1510	CH ip bend in phase sym	

Table 3. *Cont.*

Wavenumber (cm^{-1})	IR Assignments	Raman Assignments
1596		CH ip bend in phase asym
1599	C=C stretch in phenol sym	
1608		C=C stretch in phenol asym
1612	C=C stretch in phenol sym	
2911		C=C stretch in phenol asym
3021	Sym CH str on C-CH_2-C	
3038		Asym CH str on C-CH_2-C
3056	OH ip str	
3062		OH op str

a and **b** are not assigned/assignable to specific vibrational modes in the literature.

3.2. IR and Raman Dual Modality

Spectroscopic data provide critical structural information on *bis*-phenol compounds. The simplest value of dual modality is that relevant wavenumbers can be present only in IR or only in Raman. The bis-phenol moiety contains two ring hydroxyl groups; yet compelling evidence of OH stretching in the IR region is absent. Because the oxygen atom is in the same plane as the ring, asymmetric OH stretching corresponds to H stretching above or below the ring, and symmetric OH stretching is H stretching in plane with the ring. Two symmetrical OH stretching modes in sync (and 180 degrees out of phase) can explain the absence of OH stretching in the IR spectra of BPA, BPS, and BPF; the corresponding Raman peaks (3066 cm^{-1}, 3070 cm^{-1}, and 3056 cm^{-1}) are different from each other.

We found other wavenumbers which are even stronger unique fingerprints for distinguishing among these three compounds (Figure 5). In BPA, the IR peak at 1508 cm^{-1} has a very high normalized intensity versus the corresponding Raman peak. The ratio is 10.6 times larger in BPA in IR than in Raman; in BPF, the ratio is only 2.8 times larger; in BPS, the ratio is 0.57 (i.e., the Raman peak instead is 1.8 larger). In BPS, at 721 cm^{-1}, the ratio is 7.4 times larger than in Raman. In contrast with BPA, the ratio is 1.7 times larger, and in BPF, the ratios are similar (0.93). In BPS, also at 1099 cm^{-1}, the ratio is 1.9 times larger than in Raman. In BPA, the ratio is 0.37 (the Raman peak is 2.7 times larger) and in BPF, the ratio is 5.1 times larger. In BPF, the Raman signal at 845 cm^{-1} is 6.3 times greater than in the IR spectrum. In BPA and BPS, the corresponding peaks between Raman and IR are of similar intensity.

The specific vibrational modes unique to BPA, BPS, and BPF can be assigned quite precisely. For BPA, 1508 cm^{-1} corresponds to 1512 cm^{-1} assignable to in-plane in-phase bending at three adjacent sites [3 (C-H ip bend in phase)]. Since the structure is a *bis*-phenol, vibrational modes on each molecule include six molecular sites. For BPF, the normalized relative intensity is 2.8, i.e., C-H ip bend in-phase can be assigned to only one of the phenol rings. For BPS, no peak in that wavenumber indicates that neither of the rings includes 3 (C-H ip bend in phase). The closest wavenumber to a peak in that spectral range corresponds to asymmetric C-C stretching: the intensity of the Raman peak is twice as large as in IR.

For BPS, the wavenumbers 720 cm^{-1} and 1099 cm^{-1} correspond to a set of vibrational modes that can occur concurrently. The first wavenumber C-C-C ip bend (734 cm^{-1}) assigns three adjacent carbon atoms (excluding C4) in bending in-plane in sync. Three different C-C-C sites can bend in-plane in the same phenol ring or six per two phenol rings. The second wavenumber (1134 cm^{-1}) corresponds to in-phase C-H bending at C4 and occurs only once per ring. The normalized relative intensity ratio of two supports that this vibrational mode is occurring symmetrically and concurrently on both rings. In contrast, for BPA, the normalized relative intensity suggests that the first three-carbon bending mode occurs only once on each ring and the vibrational modes remain symmetrical. For BPF, the ratio IR to Raman is essentially one.

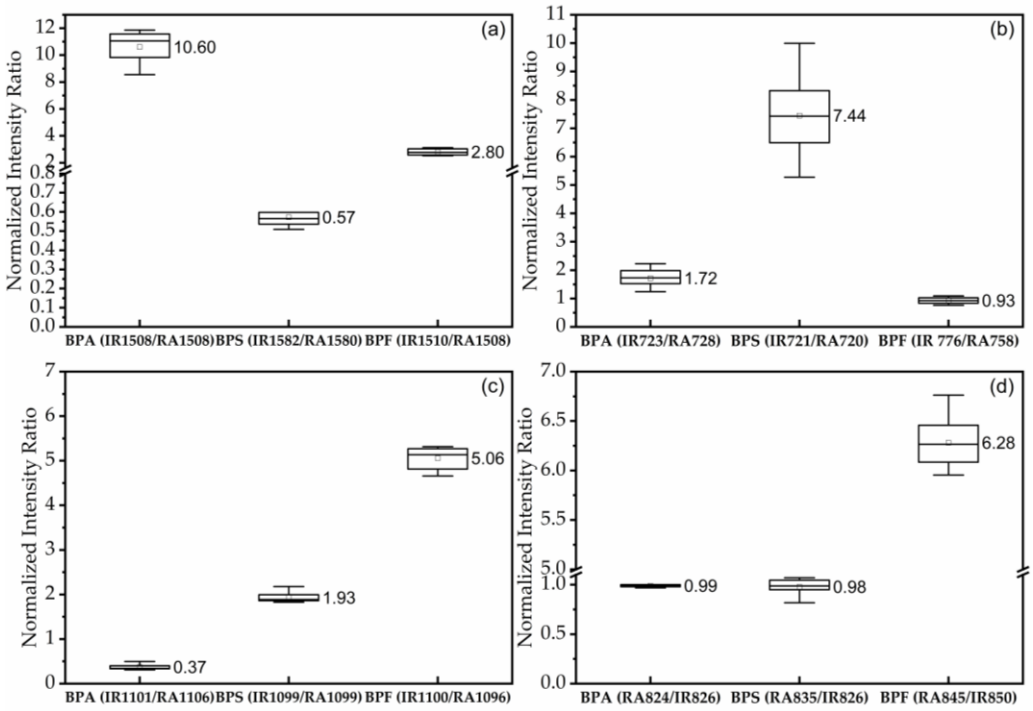

Figure 5. Unique dual-modality fingerprint wavenumbers for distinguishing BPA (**a**), BPS (**b**,**c**), and BPF (**d**).

For BPF, the wavenumber 845 cm^{-1} can be assigned to 840 cm^{-1} C-C-C trigonal bending which is a Raman frequency. The IR wavenumber 850 cm^{-1} is assigned to C-C-C puckering. This is evidence that in BPF on both rings, trigonal bending is likely occurring concurrently at three sites in each ring. The normalized intensity ratio is six. In both BPA and BPS, both C-C-C trigonal bending and C-C-C puckering are roughly of equal intensity, so neither of these modes shows a significant spectral signature.

4. Discussion

Dual-modality analysis enables addressing exactly the wavenumbers in which IR and Raman spectra are most different. In mono-modality analysis, the presence of specific wavenumbers is used in IR as evidence of identity, except that the absence of a different specific wavenumber in an IR spectrum is not equally taken as evidence against its identification. Grace et al. [18] calculated discrete vibrational modes, each having a correspondingly discrete and identifying wavenumber for a phenolic ring, not that all of them will occur at equal intensity simultaneously. Our analysis found that the major phenolic ring vibrational mode intensities in BPA, BPS, and BPF are highly significantly different, sufficient to identify one from the other despite their structural similarity.

A spectral signature for other *bis*-moieties X-A-X in BPA, BPS, and BPF (CH_3-C-CH_3, O-S-O, and H-C-H) occurs as two peaks (1620 cm^{-1} to 1580 cm^{-1}), which are assignable to X-A-X symmetrical scissoring and essentially "asymmetrical" scissoring. In each of the three, the two peaks appear to have variable intensities in IR versus Raman spectra. Asymmetric in this case refers to the vibrational mode in which X is transiently deformed as different from the other X site. The O-S-O moiety is the most rigid (i.e., also is O=S=O), so the actual "asymmetrical" scissoring sites could be at the C-S-C site instead, suggesting that the BPS vibrational modes would be the most symmetrical. BPA scissoring, the easiest to understand, involves methyl groups moving regularly towards and away from each other. Symmetrical scissoring is with H-C stretching modes in each X group *in sync*, and "asymmetrical" scissoring is with H-C stretching modes *out of sync*. Spectroscopic evidence is that BPF is the least symmetrical molecule of the three: X-A-X in H-C-H more often bends

or twists than scissors. The difference in scissoring at site A appears relevant in explaining the difference in the *bis*-phenolic portions of the three spectra.

Dual modality enables interpreting the wavenumbers in which the IR and Raman spectra are most different (in normalized relative intensity). BPA, BPS, and BPF are clearly and cleanly distinguishable despite their otherwise quite similar chemical structure. Dual-modality measurements in which specific wavenumbers are strong in one mode and absent/much weaker in the other in each case were highly statistically significant.

These plasticizers are commercially present in plastics, resulting in binary matrices of BPA, BPS, and BPF with polymer. Future research is needed to explore the same compounds in more complicated matrices.

Author Contributions: Conceptualization, K.C. and W.S.; methodology, K.C.; data curation, K.C. and F.T.; writing—original draft preparation, W.S. and K.C.; writing—review and editing, J.Q. and M.K. All authors have read and agreed to the published version of the manuscript.

Funding: This research received no external funding.

Institutional Review Board Statement: Not applicable.

Informed Consent Statement: Not applicable.

Data Availability Statement: The data presented in this study are available on request from the corresponding author. The data are not publicly available due to privacy.

Conflicts of Interest: The authors declare no conflicts of interest.

References

1. Cao, X.L.; Corriveau, J. Migration of bisphenol A from polycarbonate baby and water bottles into water under severe conditions. *J. Agric. Food Chem.* **2008**, *56*, 6378–6381. [CrossRef] [PubMed]
2. Le, H.H.; Carlson, E.M.; Chua, J.P.; Belcher, S.M. Bisphenol A is released from polycarbonate drinking bottles and mimics the neurotoxic actions of estrogen in developing cerebellar neurons. *Toxicol. Lett.* **2008**, *176*, 149–156. [CrossRef]
3. Vandenberg, L.N.; Hauser, R.; Marcus, M.; Olea, N.; Welshons, W.V. Human exposure to bisphenol A (BPA). *Reprod. Toxicol.* **2007**, *24*, 139–177. [CrossRef]
4. Morrissey, R.E.; George, J.D.; Price, C.J.; Tyl, R.W.; Marr, M.C.; Kimmel, C.A. The developmental toxicity of bisphenol A in rats and mice. *Fundam. Appl. Toxicol.* **1987**, *8*, 571–582. [CrossRef] [PubMed]
5. Welshons, W.V.; Thayer, K.A.; Judy, B.M.; Taylor, J.A.; Curran, E.M.; vom Saal, F.S. Large effects from small exposures: I. Mechanisms for endocrine-disrupting chemicals with estrogenic activity. *Environ. Health Perspect.* **2003**, *111*, 994–1006. [CrossRef]
6. Hafezi, S.A.; Abdel-Rahman, W.M. The Endocrine Disruptor Bisphenol A (BPA) Exerts a Wide Range of Effects in Carcinogenesis and Response to Therapy. *Curr. Mol. Pharmacol.* **2019**, *12*, 230–238. [CrossRef]
7. Roschi, E.; Gellini, C.; Ricci, M.; Sanchez-Cortes, S.; Focardi, C.; Neri, B.; Otero, J.; López-Tocón, I.; Smulevich, G.; Becucci, M. Surface-enhanced Raman spectroscopy for bisphenols detection: Toward a better understanding of the analyte–nanosystem interactions. *Nanomaterials* **2021**, *11*, 881. [CrossRef] [PubMed]
8. Qiu, L.; Liu, Q.; Zeng, X.; Liu, Q.; Hou, X.; Tian, Y.; Wu, L. Sensitive detection of bisphenol A by coupling solid phase microextraction based on monolayer graphene-coated Ag nanoparticles on Si fibers to surface enhanced Raman spectroscopy. *Talanta* **2018**, *187*, 13–18. [CrossRef]
9. Lin, P.Y.; Hsieh, C.W.; Hsieh, S. Rapid and sensitive SERS detection of bisphenol A using self-assembled graphitic substrates. *Sci. Rep.* **2017**, *7*, 16698. [CrossRef] [PubMed]
10. Rochester, J.R.; Bolden, A.L. Bisphenol S and F: A systematic review and comparison of the hormonal activity of bisphenol A substitutes. *Environ. Health Perspect.* **2015**, *123*, 643–650. [CrossRef]
11. Dhakal, S.; Chao, K.; Schmidt, W.F.; Qin, J.; Kim, M.; Chan, D. Evaluation of turmeric powder adulterated with metanil yellow using FT-Raman and FT-IR spectroscopy. *Foods* **2016**, *5*, 36. [CrossRef] [PubMed]
12. Dhakal, S.; Schmidt, W.F.; Kim, M.; Tang, X.; Peng, Y.; Chao, K. Detection of additives and chemical contaminants in turmeric powder using FT-IR spectroscopy. *Foods* **2019**, *8*, 143. [CrossRef] [PubMed]
13. Schmutzler, M.; Beganovic, A.; Böhler, G.; Huck, C.W. Methods for detection of pork adulteration in veal product based on FT-NIR spectroscopy for laboratory, industrial and on-site analysis. *Food Control* **2015**, *57*, 258–267. [CrossRef]
14. Almeida, M.R.; Oliveira, K.D.S.; Stephani, R.; de Oliveira, L.F.C. Fourier-transform Raman analysis of milk powder: A potential method for rapid quality screening. *J. Raman Spectrosc.* **2011**, *42*, 1548–1552. [CrossRef]
15. Guelpa, A.; Marini, F.; du Plessis, A.; Slabbert, R.; Manley, M. Verification of authenticity and fraud detection in South African honey using NIR spectroscopy. *Food Control* **2017**, *73*, 1388–1396. [CrossRef]

16. Rohman, A.; Man, Y. Application of Fourier transform infrared (FT-IR) spectroscopy combined with chemometrics for authentication of cod-liver oil. *Vib. Spectrosc.* **2011**, *55*, 141–145. [CrossRef]
17. Rohman, A.; Man, Y. Application of Fourier Transform Infrared Spectroscopy for Authentication of Functional Food Oils. *Appl. Spectrosc. Rev.* **2012**, *47*, 1–13. [CrossRef]
18. Grace, L.I.; Cohen, R.; Dunn, T.M.; Lubman, D.M.; de Vries, M.S. The R2PI Spectroscopy of Tyrosine: A Vibronic Analysis. *J. Mol. Spectrosc.* **2002**, *215*, 204–219. [CrossRef]
19. Ullah, R.; Wang, X. Raman spectroscopy of Bisphenol 'S' and its analogy with Bisphenol 'A' uncovered with a dimensionality reduction technique. *J. Mol. Struct.* **2019**, *1175*, 927–934. [CrossRef]
20. Buzgar, N.; Buzatu, A.; Sanislav, I.V. The Raman study on certain sulfates. *Ann. Stiint. Univ.* **2009**, *55*, 5–23.
21. Hernandez, B.; Pflueger, F.; Adenier, A.; Kurglik, S.G.; Ghomi, M. Vibrational analysis of amino acids and short peptides in hydrated media. VIII. Amino acids with aromatic side chains: L-phenylalanine, L-tyrosine and L-tryptphan. *J. Phys. Chem.* **2010**, *114*, 15319–15330. [CrossRef] [PubMed]